Electronic Supplementary Material (ESI) for Lab on a Chip.

Supplementary Materials for

Automated biophysical classification of apoptotic pancreatic cancer cell subpopulations by using machine learning approaches with impedance cytometry

Carlos Honrado, Armita Salahi, Sara J. Adair, John H. Moore, Todd W. Bauer, Nathan S. Swami*

*Corresponding author. Email: nswami@virginia.edu

This PDF file includes:

A. Supplementary Results

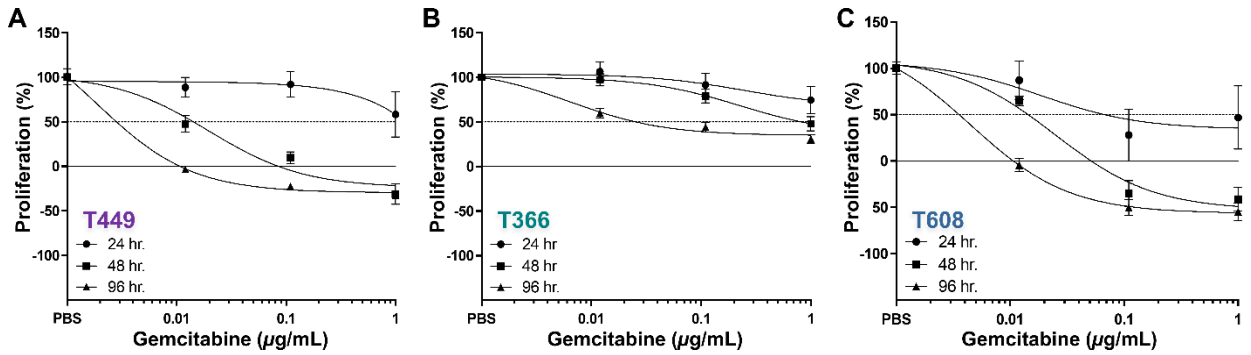

Figure S1: Proliferation studies on PDAC cell lines: A - T449, B – T366, and C – T608. Cell cultures were exposed to varying concentrations of gemcitabine (0.01, 0.1, and 1 μg mL^{-1}) for: 24 h (circle), 48 h (square) and 96 h (triangle). Proliferation (%) is calculated as the relative proliferation under each treated condition compared with untreated for each exposure period and gemcitabine concentration.

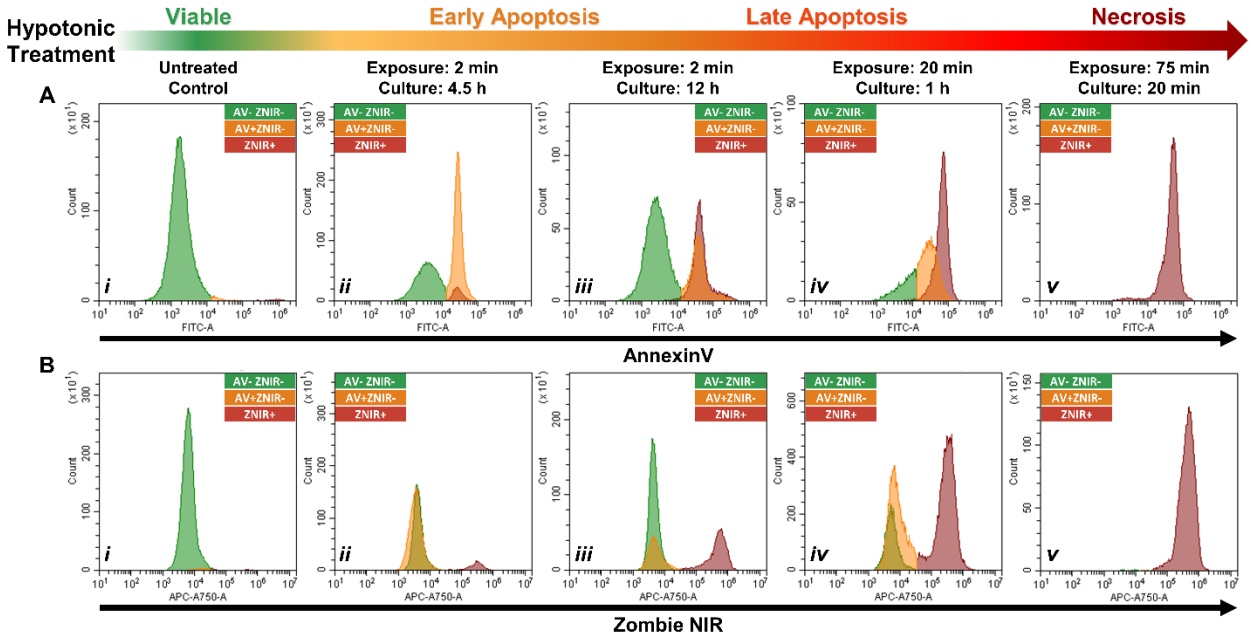

Figure S2: Hypotonic treatment studies on PDAC T449 cell line. Histograms A – Annexin V (AV) and B – Zombie Near-Infrared (ZNIR) show that exposing cell cultures to DI water for increasing periods of time induces cells towards apoptosis and necrosis pathways.

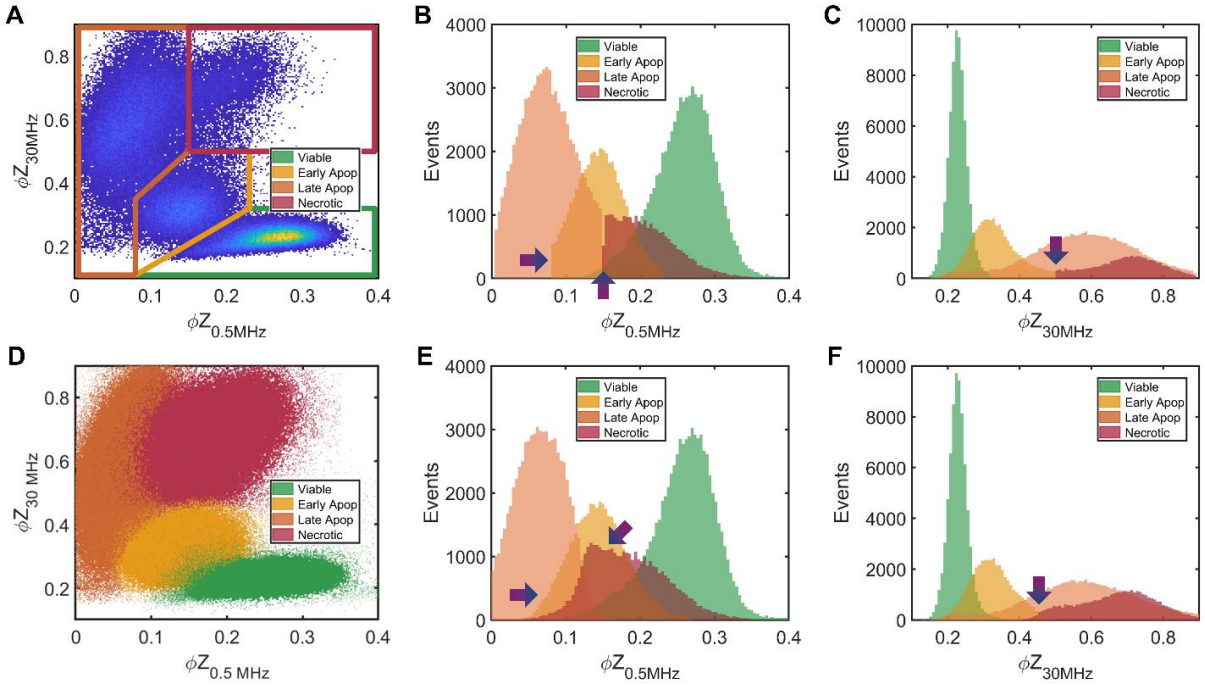

Figure S3: Manual gating versus clustering with unsupervised learning. A – Manual gates for each viability subpopulation applied to the density scatter plot of impedance phase at 0.5 MHz ($\boldsymbol{\phi}Z_{0.5MHz}$) versus impedance phase at 30 MHz ($\boldsymbol{\phi}Z_{30MHz}$) for merged data from the different hypotonic treatment samples. Histograms for B – $\boldsymbol{\phi}Z_{0.5MHz}$ and C – $\boldsymbol{\phi}Z_{30MHz}$ of the manually gated subpopulations. D – A Gaussian Mixture Model (GMM), with k = 4 clusters, applied to cluster each viability subpopulation in the density scatter plot of impedance phase at 0.5 MHz ($\boldsymbol{\phi}Z_{0.5MHz}$) versus impedance phase at 30 MHz ($\boldsymbol{\phi}Z_{30MHz}$) for merged data from the different hypotonic treatment samples. Histograms for E – $\boldsymbol{\phi}Z_{0.5MHz}$ and F – $\boldsymbol{\phi}Z_{30MHz}$ of the machine learning gated subpopulations.

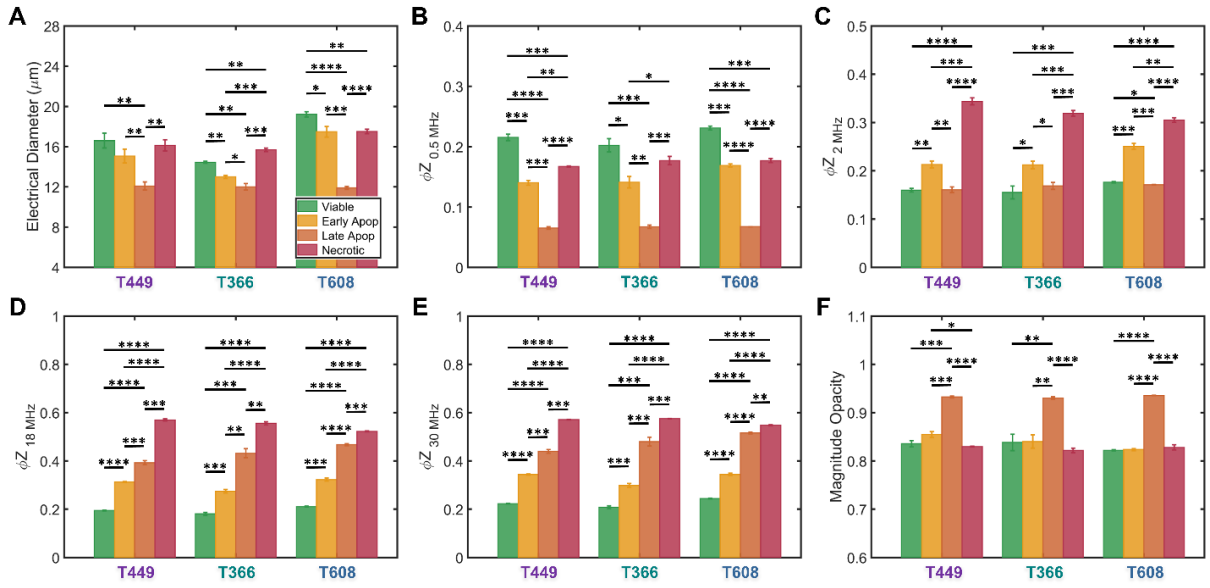

Figure S4: Comparison of the impedance cytometry biometrics of electrical diameter (A), impedance phase at 0.5 MHz ($\boldsymbol{\phi}Z_{0.5MHz}$, B), at 2 MHz ($\boldsymbol{\phi}Z_{2MHz}$, C), at 18 MHz ($\boldsymbol{\phi}Z_{18MHz}$, D) and

at 30 MHz ($\boldsymbol{\phi}Z_{30MHz}$, E), and magnitude opacity ($|Z|_{2MHz}$ / $|Z|_{0.5MHz}$, F) for each untreated PDAC cell line (n = 3). Statistical significance: *p ≤ 0.05 ; **p ≤ 0.01, ***p ≤ 0.001 and ****p ≤ 0.00001.

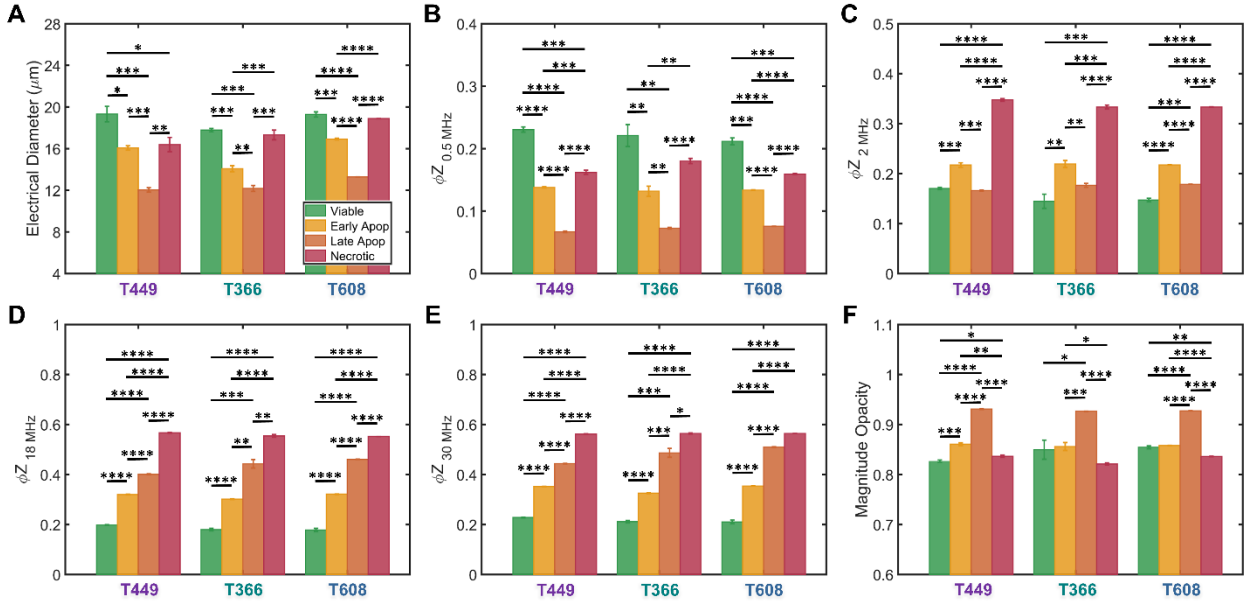

Figure S5: Comparison of the impedance cytometry biometrics of electrical diameter (A), impedance phase at 0.5 MHz ($\boldsymbol{\phi}Z_{0.5MHz}$, B), at 2 MHz ($\boldsymbol{\phi}Z_{2MHz}$, C), at 18 MHz ($\boldsymbol{\phi}Z_{18MHz}$, D) and at 30 MHz ($\boldsymbol{\phi}Z_{30MHz}$, E), and magnitude opacity ($|Z|_{2MHz}$ / $|Z|_{0.5MHz}$, F) for each gemcitabine-treated PDAC cell line (n = 3). Statistical significance: *p ≤ 0.05 ; **p ≤ 0.01, ***p ≤ 0.001 and ****p ≤ 0.00001.

B. Supplementary Methods

Dielectric Shell Modelling

For the case where a particle is suspended in a dielectric medium, dielectric spectroscopy can be used to measure the dielectric properties of the suspension[1]. This mixture of particle and medium can be approximated to that of a single dispersion using Maxwell's mixture theory (MMT)[2]. MMT can be used to combine the dielectric properties of all parts into an overall complex permittivity of the mixture ($\tilde{\varepsilon}_{mix}$):

$$\tilde{\varepsilon}_{mix} = \tilde{\varepsilon}_{medium}\left(1 + 3\,\varphi\,\tilde{f}_{CM,mix}\right) \qquad \text{(S1)}$$

where $\tilde{\varepsilon}_{medium}$ is the complex permittivity of the suspending medium, φ the volume fraction of the particle in the medium, and $\tilde{f}_{CM,mix}$ the Clausius−Mossotti factor of the cell in the mixture. In practical terms, $\tilde{\varepsilon}_{mix}$ describes the change in the medium permittivity, due to the presence of a particle of a given volume and can only be used if the volume fraction is small, *i.e.*, $\varphi \ll 1$. For the case of a cell in suspending medium, MMT-based, shell models can be used to retrieve the dielectric properties of the cell[3–5]. While cells have an intricate internal structure surrounded by a membrane, a simplified approximation can be used based on shell models, wherein a cell is described as a series of *n* concentric shells with defined dielectric properties (**Figure S6A**). In a standard single-model, there are two dispersions, corresponding to the existing interfaces, i.e. medium-membrane and membrane-interior.

For a shell model, the Clausius−Mossotti factor of the cell in the mixture is given by:

$$\tilde{f}_{CM,mix} = \frac{\tilde{\varepsilon}_{particle} - \tilde{\varepsilon}_{medium}}{\tilde{\varepsilon}_{particle} + 2\tilde{\varepsilon}_{medium}} \quad \text{(S2)}$$

The complex permittivity of the cell, $\tilde{\varepsilon}_{particle}$, is an aggregation of the complex permittivities of all the *n* shells modelled for the particle, and represents the final dispersion, typically corresponding to medium and cell membrane. The complex permittivity of any dispersion can be calculated as:

$$\tilde{\varepsilon}_{n,n+1} = \tilde{\varepsilon}_n \frac{\gamma_{n-1,n}{}^3 + 2\left(\frac{\tilde{\varepsilon}_{n+1} - \tilde{\varepsilon}_n}{\tilde{\varepsilon}_{n+1} + 2\tilde{\varepsilon}_n}\right)}{\gamma_{n-1,n}{}^3 - \left(\frac{\tilde{\varepsilon}_{n+1} - \tilde{\varepsilon}_n}{\tilde{\varepsilon}_{n+1} + 2\tilde{\varepsilon}_n}\right)} \quad \text{(S3)}$$

with,

$$\gamma_{n-1,n} = \frac{r_{n-1}}{r_n} \quad \text{(S4)}$$

where r is the radius of the shell being modeled. The complex permittivities of each specific shell can in turn be calculated using:

$$\tilde{\varepsilon}_n = \varepsilon_o \varepsilon_n - i\frac{\sigma_n}{\omega} \quad \text{(S5)}$$

where ε_n and σ_n can be ranges of permittivities and conductivities, respectively, being tested with the model for each *n* shell; while ε_0 is the constant vacuum permittivity (8.85×10^{-12} F m^{-1}) and ω is the angular frequency along the frequency spectrum measured. By calculating of each shell, and using **Equation S1**, it is then possible to calculate the dielectric decrement due to the presence of the particle in the suspending medium between the measurement electrodes. Thus, the impedance of the mixture ($\tilde{Z}_{mix}$) can be obtained:

$$\tilde{Z}_{mix} = {}^{1}/_{i\omega\tilde{\varepsilon}_{mix}G_f} \quad \text{(S6)}$$

where $i^2 = -1$, ω is the angular frequency, and G_f is the geometric constant of the system. For an ideal parallel plate electrode system, G_f is simplified to $\mathrm{A}_{electrode}/\mathrm{d}_{electrode}$, where $\mathrm{A}_{electrode}$ is the electrode surface area and $\mathrm{d}_{electrode}$ is the separation distance between electrodes.

Given the frequency-dependence of $\tilde{Z}_{mix}$, relaxation curves for the impedance magnitude and phase can be calculated using:

$$\left|\tilde{Z}_{mix}\right| = \sqrt{\mathrm{Re}\left(\tilde{Z}_{mix}\right)^2 + \mathrm{Im}\left(\tilde{Z}_{mix}\right)^2} \quad \text{(S7)}$$

$$\phi\tilde{Z}_{mix} = \arctan\left(\frac{\mathrm{Im}(\tilde{Z}_{mix})}{\mathrm{Re}(\tilde{Z}_{mix})}\right) \quad \text{(S8)}$$

An iterative algorithm can be implemented to calculate these curves for a wide spectrum of combinations between different electrophysiology metrics (e.g. varying particle size, membrane conductivity or internal conductivity; **Figure S6B-F**).

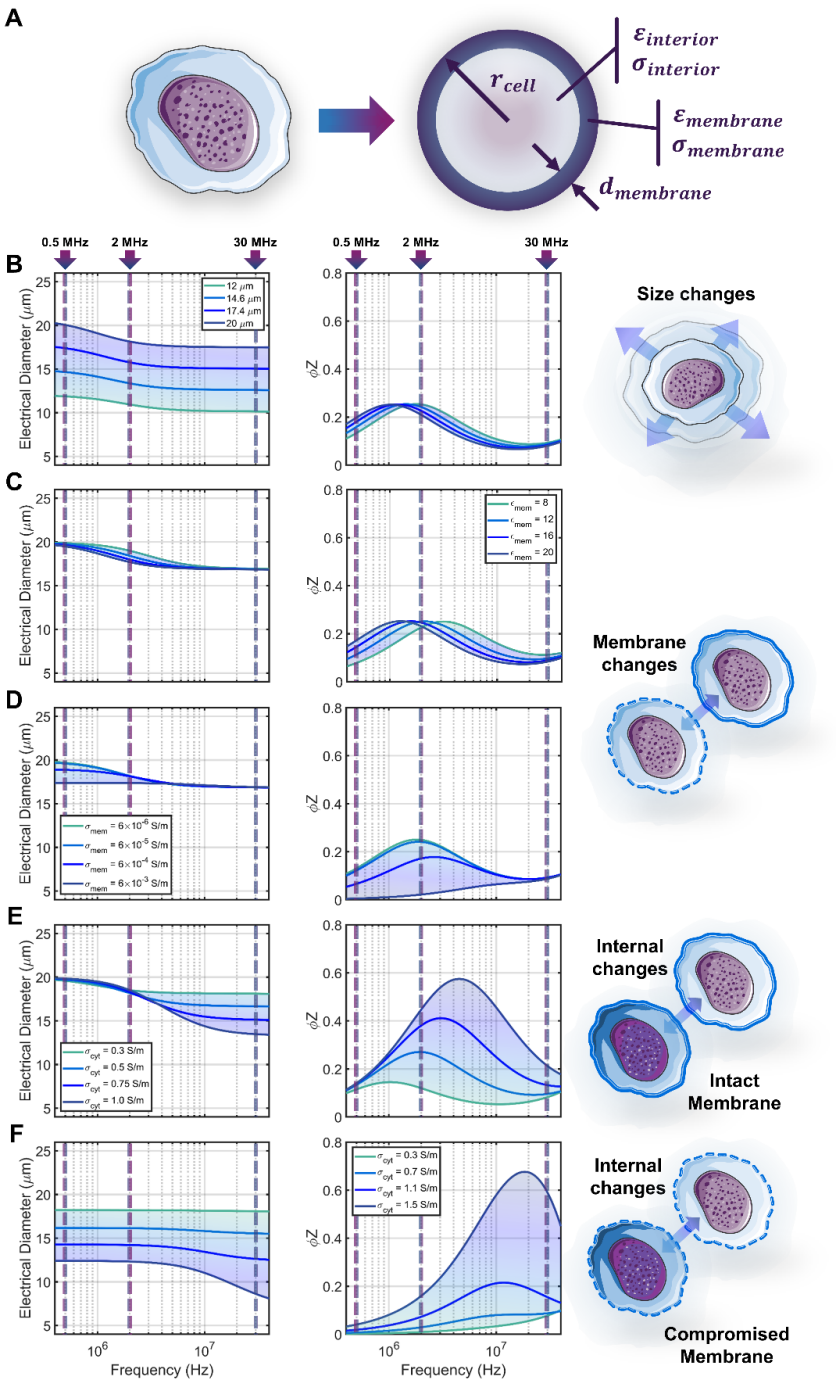

Figure S6: Dielectric shell modelling. A – An equivalent single-shell model of a biological cell in a suspending medium, obtained through Maxwell's mixture theory. Modelled electrical diameter and impedance phase ($\boldsymbol{\phi}$Z) for a variety of different alterations to the dielectric properties: B – cell size ($\boldsymbol{r_{cell}}$ from 6 to 10 µm, C – membrane permittivity ($\boldsymbol{\varepsilon_{mem}}$ from 8 to 20), D – membrane conductivity ($\boldsymbol{\sigma_{mem}}$ from 6×10^{-6} to 6×10^{-3}), E – internal conductivity ($\boldsymbol{\sigma_{int}}$ from 0.3 to 1.0 S m^{-1}, assuming $\boldsymbol{\varepsilon_{mem}}$ = 14 and $\boldsymbol{\sigma_{mem}}$ < 1×10^{-6} S m^{-1}) , and F – internal conductivity ($\boldsymbol{\sigma_{int}}$ from 0.3 to 1.5 S m^{-1}, assuming $\boldsymbol{\varepsilon_{mem}}$ = 14 and $\boldsymbol{\sigma_{mem}}$ = 6×10^{-3} S m^{-1}). Cells modelled using a single-shell model with the following set of dielectric properties (if not being varied at each

individual sub-figure case): $\boldsymbol{d_{mem}}$ = 10 nm, $\boldsymbol{\varepsilon_{mem}}$ = 14, $\boldsymbol{\sigma_{mem}}$ < 1 × 10^{-6} S m^{-1}, $\boldsymbol{\varepsilon_{int}}$ = 60, $\boldsymbol{\sigma_{int}}$ = 0.5 S m^{-1}, $\boldsymbol{\varepsilon_{medium}}$ = 80, $\boldsymbol{\sigma_{medium}}$ = 1.6 S m^{-1}, $\boldsymbol{d_{electrode}}$ = 50 µm, $\boldsymbol{A_{electrode}}$ = 2.5 × 10^{-9} m^2.

References

1. Morgan, H. & Green, N. G. *AC Electrokinetics: colloids and nanoparticles*. (Research Studies Press Ltd., 2002).
2. Maxwell, J. C. *A treatise on electricity and magnetism*. *A treatise on electricity and magnetism* **1**, (Clarendon Press, 1881).
3. Hanai, T., Koizumi, N. & Irimajiri, A. A method for determining the dielectric constant and the conductivity of membrane-bounded particles of biological relevance. *Biophys. Struct. Mech.* **1**, 285–294 (1975).
4. Huang, Y., Hölzel, R., Pethig, R. & Wang, X. B. Differences in the AC electrodynamics of viable and non-viable yeast cells determined through combined dielectrophoresis and electrorotation studies. *Phys. Med. Biol.* **37**, 1499–1517 (1992).
5. Irimajiri, A., Hanai, T. & Inouye, A. A dielectric theory of 'multi-stratified shell' model with its application to a lymphoma cell. *J. Theor. Biol.* **78**, 251–269 (1979).